Evolution of self-organized two-dimensional patterns of nanoclusters through demixing

Madhumita Choudhuri, A. N. Sekar Iyengar, Alokmay Datta, and M. S. Janaki

Phys. Rev. E **92**, 032907 — Published 14 September 2015

DOI: 10.1103/PhysRevE.92.032907

Evolution of self-organized two-dimensional patterns of nano-clusters through de-mixing

Madhumita Choudhuri,[1] A.N. Sekar Iyengar,[2] Alokmay Datta,[1,*] and M.S.Janaki[2]

[1] *Surface Physics and Material Science Division, Saha Institute of Nuclear Physics, 1/AF Bidhannagar, Kolkata 700064, India*
[2] *Plasma Physics Division, Saha Institute of Nuclear Physics, 1/AF Bidhannagar, Kolkata 700064, India*

A mixture of dodecanethiol-capped Au nanoparticles (AuNPs) and the amphiphilic fatty-acid Stearic Acid (StA), spread as a monomolecular layer on water surface, is observed with Brewster Angle microscopy (BAM) to form a two-dimensional network of AuNP clusters through de-mixing, at concentration of AuNPs by weight, $(\overline{p}) > 10\%$ and the surface pressure, $(\pi) \geq 10$ mN m^{-1}. For $\pi = 15$ mN m^{-1}, the number of nodes (n) remains unchanged till ~ 2 hours and then changes over to a lower n state, where the pattern consists of almost perfect circles with greater in plane thickness of the AuNP lamellae. For the higher n state the mean square fluctuation of BAM intensity remains flat and then decays as $f(\xi) = \xi^{2\alpha}$ with $\alpha \sim 0.6$ (correlated fluctuations) over the length scales of 400 μm-6 μm and below 6μm, respectively. For the lower n state the fluctuation decays almost over the entire length scale with $\alpha = 0.3$, indicating emergence of aperiodicity from quasi-periodicity and a changeover to anti-correlated fluctuations. These patterns can be looked at as two distinct chaotic trajectories in the $I - I'$ 'phase space' of the system (I being the scattered light intensity at any position of the pattern and I' its gradient) with characteristic Lyapunov exponents.

PACS numbers: 82.40.Bj; 81.16.Rf; 05.65.+b; 68.18.-g.

I. INTRODUCTION

Patterns, in general, form through processes of self organization in systems that are driven far from equilibrium [1–3]. In addition to understanding the underlying thermodynamics and mechanisms involved in pattern formation, patterns are also studied within the formalism of universality classes, fractals and self similarity, criticality and percolation, chaos and complexity [4, 5]. Such pattern formation is, in a number of instances, guided by the competing tendencies of integration and segregation of constituents in mixtures with long-term instabilities [6] and hence studies of patterns on a long timescale are important.

Self-organization of AuNPs has been reported in various polymer/lipid matrices [7–11]. These include both in situ studies at the air-water interface and ex situ ones after transferring the film onto a substrate. In all these the focus was on the morphology of the self-organized structures on a scale of μm to nm. However, to our knowledge, the evolution of such patterns over a timescale spanning more than say, 2hrs, has not been studied, perhaps due to the apparent stability of the pattern.

Here we present a maiden study of the long-term dynamics of one such spatial pattern resulting from the self-organization of dodecanethiol-capped gold nanoparticles (AuNPs) in a monomolecular film of the amphiphilic fatty acid, stearic acid (StA) at air-water interface. In a previous communication we gave a preliminary report on the formation of a spatial pattern of AuNPs in stearic acid featuring an interconnected network of enclosed micro-spaces [12]. In that work the pattern was characterized by measuring the average pore size of the interconnected microspaces and studied while varying the surface pressure π. Since it was the first observation of such a network the emphasis was on the reproducibility and reversibility of the pattern in general and during compression-decompression cycles in particular. Most important, however, is that we did not carry out any study at timescales longer than 2 hours and hence, no really long-term dynamics was investigated.

The major aspect of the present study is precisely this long-term observation exceeding 4 hours, whereby *an entirely new pattern or state* has been found to emerge after 2 hours. In this communication we have characterized the patterns by the *node density*, n, a more accurately measureable quantity, in order to carry out a rigourous and extensive study of long term dynamics of this 2D pattern as a function of n, from its initial to final state with surface pressure as a fixed parameter. Our presentation of this long-term dynamics of the pattern includes statistical analyses of the pattern in its initial and finally evolved states where the two states have been studied within the context of statistical fluctuations, correlations over real space and the corresponding power spectra in reciprocal space [13]. The initial state has been identified to be quasiperiodic and the final state to be completely aperiodic, while both the states are found to be spatially chaotic through a calculation of the Lyapunov exponents. In a 2D system such as ours fluctuations play a major role and indeed we have shown that the pattern evolves from one chaotic state to another [14–16] through a change in the nature of this fluctuation.

* alokmay.datta@saha.ac.in

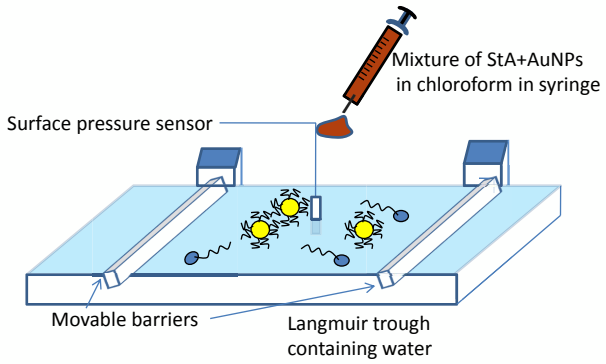

FIG. 1. (Color online) Schematic of the experiment showing the Langmuir trough with movable trough barriers. Au nanoparticles (AuNPs) are depicted as spheres with surrounding thiol caps while the StA molecules have hydrophillic spherical head groups and hydrophobic tails.

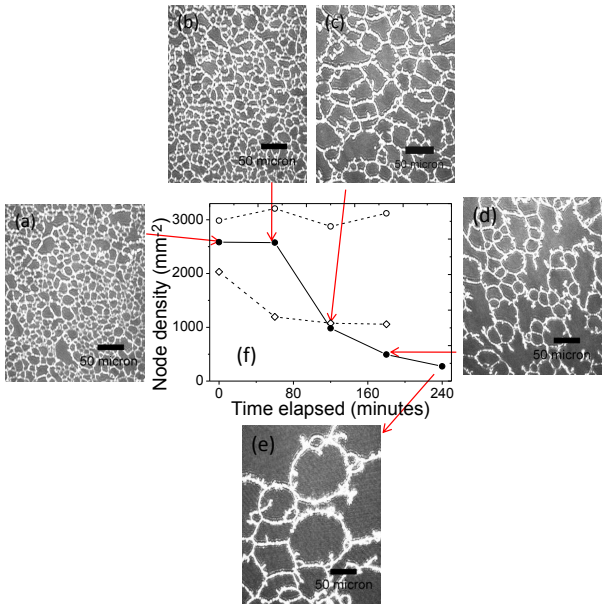

FIG. 2. (Color online) Brewster Angle Microscopy (BAM) images of the Dodecanethiol-capped Au Nanoparticle (AuNP) (20% by wt) - Stearic Acid (StA) mixed thin film at Surface Pressure (π)=15 mN m^{-1} at (a) 0, (b) 60, (c) 120, (d) 180 and (e) 240 min (scan size 432μm $\times$ 337μm). AuNP clusters appear as bright white threads on the StA monolayer forming the dark grey background. (f) Variation of node density (nodes per mm^2, n, $\bullet$) of the pattern with time. Data in $\circ$ and $\diamond$ represent monolayers with 30% Au and $\pi = 10$ mN m^{-1} and 20 mN m^{-1}, respectively.

II. EXPERIMENTAL DETAILS

AuNPs were synthesized by Brust's method [17, 18] and consisted of spherical Au cores each 2-3 nm wide surrounded by a capping layer of hydrophobic dodecane thiol, as checked by Transmission Electron Microscopy[12]. 50μl of a chloroform solution of AuNPs (<1 mol% of mixture) and StA, was spread at the surface of aspirated, purified water (Millipore, resistivity 18 MΩcm) in a Langmuir trough (NIMA Technologies UK). The AuNPs self-organize in the monolayer cushion of StA [19, 20] formed at the air-water interface (Figure 1). These NPs interact via short-ranged van der Waals attractive forces with each other as well as with the surrounding StA molecules through the alkyl chains of their thiol caps and those of the surrounding StA tails, and this attractive force stabilizes the AuNPs against complete phase segregation in the film [21, 22].

The film of StA and AuNPs so formed was compressed quasi-statically by moving in the two Teflon barriers (13 cm wide), provided in the trough, at 1 cm/min. The surface pressure π, given by $\gamma_0 - \gamma$ (where γ_0 (γ) is the surface tension of pure (monolayer-covered) water), was measured from the force acting on a Wilhemy paper plate (Whatman's Chr1 grade) suspended at the air-film interface. The film morphology was then studied with an Imaging Ellipsometer (ep3 Accurion Nanofilm GmbH, Germany) in the Brewster Angle Microscopy mode, at an in-plane resolution of 450 nm [23, 24]. The film was maintained at constant π through very slow compression of the monolayer that compensated for the loss of molecules through different mechanisms over the period of our observation. Time evolution of the film was studied once this desired surface pressure was reached whereby images of the film were acquired after every 10 minutes over a period of 4 hours.

III. RESULTS AND DISCUSSION

A. Formation of a micro-scale network pattern

The compression of the AuNP-StA film at water surface caused the AuNPs to form clusters visible at even $\pi \simeq 0$. The clusters decorated the domain boundaries between a condensed phase and a low density phase of StA, in the low pressure coexistence regime. On steady compression beyond a threshold, the density fluctuations of the AuNPs gave rise to self-organization of a 2D network pattern of AuNP clusters (Figure 2(a)) in the StA monolayer [12] with extensive monolayer coverage for concentration of AuNPs (by weight) $\overline{\rho} > 10\%$ and $\pi \geq 10$ mN m^{-1}. The pattern was found to be stable till 20 mN m^{-1} beyond which it began to collapse laterally.

B. Long time evolution of the pattern

We explored the long-time evolution of this pattern for a AuNP (20% by weight)-StA thin film at $\pi = 15$

mNm^{-1}. Figure 2(a)-(e) shows the evolution of the pattern over a period of 4 hours while Figure 2(f) shows the change in the 2D density of *nodes* (nodes per mm^2, n) connecting three (or more) AuNP lamellae, at π = 10, 15 and 20 mNm^{-1}. At π= 15 mNm^{-1} we see an initial period of stability with a pattern characterized by high n and quasiperiodicity, followed by a dramatic fall in n during the second and third hours, finally slowing down in the final fourth hour to another pattern having a lower value of n and mostly ring shaped structures with a wide distribution of diameters. This remains almost unchanged for at least 20 hours. The completely different long-term dynamics observed for different Au concentrations and π rules out any dominant role of experimental drifts. The absence of any external factor or any apparent change in the composition of the mixed monolayer in undergoing the total change in pattern from the initial to the final state does not also suggest a role of Marangoni forces.

C. Spatial Correlations and Mean square fluctuation

The spatial variation of intensity along a typical line in each of the observed patterns corresponds to spatial variations in AuNP density. The mean square (m.s) intensity fluctuation $f(\xi)$ and the power spectra $p(k)$, where ξ is the separation between points along any horizontal or vertical line in the images, k is the reciprocal of ξ and $p(k)$ the Fourier transform of intensity autocorrelation $C(\xi)$, were obtained for each of the two states in Figure 2(a) and 2(e) with

$$f(\xi) =< [\Delta I(\xi) - < \Delta I(\xi) >]^2 > \quad (1)$$

$$C(\xi) = \frac{< (I(q_0) - < I(q_0) >)(I(q_0+\xi) - < I(q_0) >) >}{< (I(q_0) - < I(q_0) >)^2 >} \quad (2)$$

where I is the reflected intensity along a typical line of the image, q is the space coordinate ($q = x$ or y), and $\Delta I(\xi) = I(q_0+\xi) - I(q_0)$. Fluctuation and power spectrum, for the high n state, are shown respectively in Figure 3(a) and 3(b) while those for the low n state are shown respectively in Figure 3(c) and 3(d). For any particular value of ξ, the averages were computed by varying q_0 over 5 lines (separated by 100 pixels) along the breadth of the image, where each line consisted of 949 pixels. $f(\xi)$ along a typical line shows for the initial high n state a more or less flat part between 432 μm ($\sim$ image width) to 6 μm ($\sim$ cell width in the network) below which it crosses over to a power law decay regime ($f(\xi) = \xi^{2\alpha}$) with an average Hurst exponent $\alpha = 0.6$ that signifies long range correlations.

For this high n state, a model periodic intensity variation with some random spacing between the pulses (Figure 4(a)) produced $f(\xi)$ and $p(k)$ (Figure 4(b) and (c)) similar to those for the observed pattern (Figure 3(a) and (b)), leading us to conclude that oscillations in the flat part of Figure 3(a) occur due to presence of periodicity, while the irregularity in the spacing of these oscillations results from random modulations, and that the initial high n state is a quasiperiodic state with random modulations embedded in spatial periodicity.

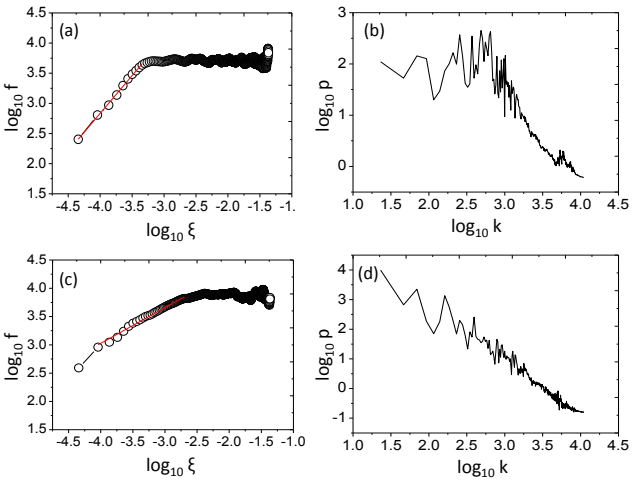

FIG. 3. (Color online) (a,c) Mean square fluctuation (*log f* vs *log* ξ) and (b,d) power spectrum (*log p* vs *log k*, $k = \xi^{-1}$) of the intensity profile along a typical line across Figure 2(a) and Figure 2(e), respectively. Red lines show power law fits. See text for details. $log \Rightarrow log_{10}$.

The fluctuations for the low n state, on the other hand, shows a reduced flat region extending only over larger lengths (432-50 μm) indicating larger structures and a single slope over almost the whole range with $\alpha = 0.3$ signifying long range anticorrelations (Figure 3(c)). The flat region consists of broad peaks at an average separation $\sim 80\mu m$ ($\sim$ size of rings). Sharp spikes in $p(k)$ of the initial state (Figure 3(b)) change to a smoother spectrum of k values (Figure 3(d)). The emergence of rings of all possible diameters at the end of long time evolution of the film destroys the initial quasi-periodicity and makes a prediction of spatial intensity variations impossible, suggesting a spatially chaotic pattern. However, the reliable parameter to quantify chaotic behavior is the Lyapunov exponent and we decided to extract it from both the states.

D. Lyapunov exponents and chaos

The Lyapunov exponent (λ) measures the rate of exponential divergence or convergence of trajectories in phase space over time[25]. A positive λ signifies chaos, i.e. divergence of two states with slightly different initial conditions with time, the magnitude of λ determining how soon the system dynamics becomes unpredictable. In the context of our system, the time series is replaced with a

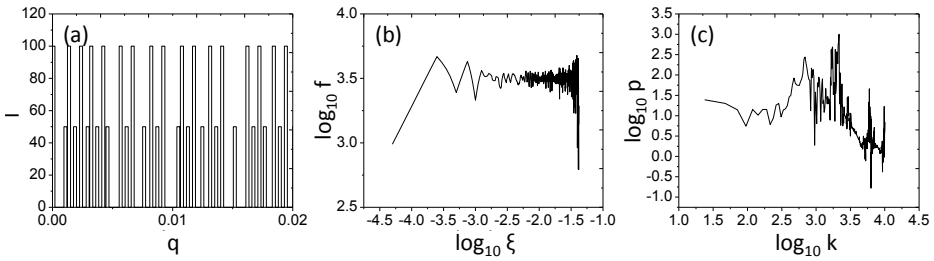

FIG. 4. (a) A quasi-periodic wave model for the pattern at T = 0 min, (b) the corresponding $f(\xi)$ and (c) $p(k)$.

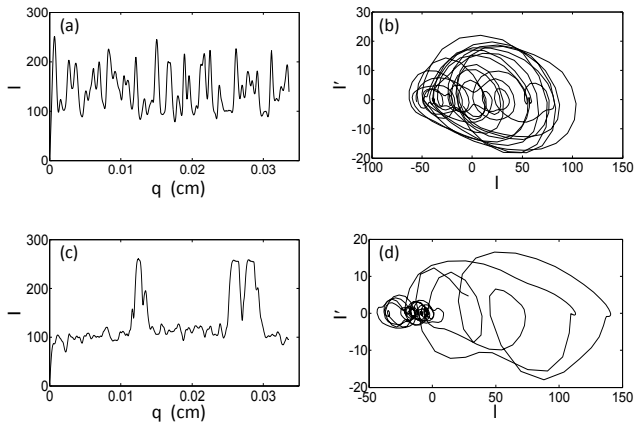

FIG. 5. (a) I vs space co-ordinate (q) and (b) spatial derivative of intensity (I') vs intensity (I) along a typical line of the observed pattern for initial high node density state, (c) I vs q and (d) I' vs I along a typical line of observed pattern for the final low node density state.

spatial series and hence λ here measures the rate of loss of predictability of intensity over space.

The Lyapunov exponents were estimated by Rosenstein's method using the TISEAN software package, which treats two very close values along the spatial series as the initial conditions for two close, perturbed trajectories [26, 27]. The distance Δ_0 between these values for a chaotic system then grows exponentially in time as $\Delta_l = \Delta_0 e^{\lambda l}$, l being the number of steps. Intensity data along successive lines along the breadth of the image were concatenated to increase data points and hence the accuracy in determining λ. After concatenating 3 successive lines of the image (949×3 data points) λ was found to saturate. This was repeated at different locations along the breadth of the images, whereupon we obtained $0.13 \leq \lambda \leq 0.19$ for the high n state and $0.13 \leq \lambda \leq 0.27$ for the low n state, indicating a small increase for the final state over the initial one.

Variations in I along typical lines of the experimental high and low node states (Figure 2(a) and (e)) are plotted in (Figure 5(a) and (c)), while spatial derivatives of I (I') against I along those lines are plotted in (Figure 5(b) and (d)), respectively. Both states have non-periodic orbits but whereas the initial state follows a trajectory filling the phase space with some closed orbits, the final state is dominated by low amplitude structures forming a dense region in the phase space with some large amplitude ones surrounding it, showing that both states have spatially chaotic but distinct natures.

E. Instability and fluctuation driven dynamics

The homogenously mixed state, thus, is a stable state only at very low surface pressure. The competition between the NP-NP cohesion on the one hand and NP-StA adhesion on the other causes a competition between aggregation and segregation of mixture constituents leading to an instability. The instability persists and is further amplified on compression because the molecules are constrained in two dimensions. Beyond a threshold the system becomes unstable to a narrow band of wave vectors resulting in a spatially quasiperiodic initial state. However, the system is only quasi-stationary in this state so that this quasiperiodic state with time gives way to an aperiodic pattern with a wider spectrum in k space. The instability may thus be classified as Type II_s of Cross and Hohenberg [2].

In most physical systems the control parameter is important and thermal effects are treated as insignificant. In contrast, for our micro-scale patterns formed by submicron sized clusters interacting via short-ranged forces, fluctuation is expected to play a determining role in pattern evolution especially if this fluctuation is correlated or anti-correlated. We propose that the final chaotic state is achieved by stochastic elements that drive the system towards it. Since the effect of fluctuation slowly builds up in the system the exact time duration after which the final chaotic state is observed varies in repeated experiments. However the final state always consists of rings of varying diameters. This formation of rings as the final state of the pattern is favored on account of closer packing of AuNP clusters accompanied by an increase in

the number of nearest and next nearest neighbors (Figure 6(a) and (b)). The strength of the short-ranged cohesive force between the AuNPs and the resistance offered to their motion by the StA monolayer ensures the stability of the initially formed high node density state for a considerable length of time. This regime is characterized by correlated fluctuations ($\alpha = 0.6$) signifying a *superdiffusive regime*.

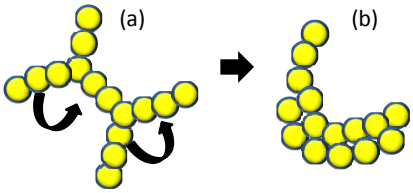

FIG. 6. (Color online) (a) Nodes of the pattern with interconnecting lamellae in the high n state, formed by AuNP clusters depicted as spheres and (b) formation of close packed structures after long time evolution resulting in the low n state of the pattern.

Fluctuations may, however, destroy nodal points and drive the system to the low node density state. That the interconnected porous network ends up with circular ring structures points towards the tendency of forming minimum enclosing perimeters favored by a reduction in line tension and formation of close packed structures without collapsing or forming Diffusion Limited Aggregates. The AuNP clusters are therefore guided by the 2D analog of the principle of minimum surfaces guiding the structure and dynamics of soap bubbles in a foam [28]. Here the fluctuations become anti-correlated ($\alpha = 0.3$) consistent with *subdiffusion*.

IV. CONCLUSION

We have studied the long-time evolution of a micro-scale pattern in two dimensions, formed by the de-mixing of two fluids, one of which is composed of nano-clusters of Au nanoparticles and the other is a Langmuir monolayer of Stearic acid (an amphiphile) wherein the pattern was found to evolve from one chaotic state to another. Fluctuations are known to be dominant in 2D systems [29–32] near equilibrium. Our results underscore the importance of correlated (or anti-correlated) fluctuations in complex fluids in two-dimensions in determining their non-equilibrium behavior. The Hurst exponents were found to be 0.6 (corresponding to a correlated signal) and 0.3 (corresponding to an anti-correlated signal) respectively for the initial and final states of the pattern indicating superdiffusive and subdiffusive de-mixing consistent with the anisotropic, superdiffusive and subdiffusive Brownian motions recently observed in complex fluids [33]. Further, our studies emphasize the importance of fluctuations in patterns formed at micro and nano-scales unlike the case of macroscopic patterns. For such micro and nano-scale patterns superdiffusive and subdiffusive de-mixing originating from correlated and anti-correlated fluctuations can cause a transition from one kind of pattern to another.

V. ACKNOWLEDGEMENTS

M. C. thanks Pankaj Shaw (S.I.N.P) for assistance, the Director (S.I.N.P) and C.S.I.R (India) for research support. We have benefited considerably from the suggestions of Professor Michail Zak, Jet Propulsion Laboratory, USA.

[1] G. Nicolis and I. Prigogine, *Self Organization in Non-Equilibrium Systems* (John Wiley and Sons, New Jersey, USA), (1977).
[2] M.C. Cross and P.C. Hohenberg, Pattern formation outside of equilibrium, Rev. Mod. Phys. **65**, 851 (1993).
[3] J.P. Gollub and J.S. Langer, Pattern formation in non equilibrium physics, Rev. Mod. Phys. **71**, 396 (1999).
[4] Per Bak, *How Nature Works* (Springer-Verlag, New York, USA), (1996).
[5] A.L. Barábasi and H.E. Stanley, *Fractal Concepts in Surface Growth* (Cambridge University Press, Cambridge, England), (1995).
[6] J.L. Barrat and J.P. Hansen, *Basic Concepts for Simple and Complex Liquids*, (Cambridge University Press, Cambridge, England), (2003).
[7] C. R. Hansen, F. Westerlund, K. Moth-Poulsen, R. Ravindranath, S. Valiyaveettil, and T. Bjørnholm, Polymer-templated self-assembly of a 2-dimensional gold nanoparticle network, Langmuir **24**, 3905 (2008).
[8] T. Hassenkam, K. Nørgaard, L. Iversen, C.J. Kiely, M. Brust, and T. Bjørnholm, Fabrication of 2D gold nanowires by self assembly of gold nanoparticles on water surfaces in the presence of surfactants, Adv. Mat. **14**, 1126 (2002).
[9] A. Mogilevsky, R. Volinsky, Y. Dayagi, N. Markovich, and R. Jelinek, Gold nanoparticle self-assembly in saturated phospholipid monolayers, Langmuir **26**, 7893 (2010).
[10] A. Mogilevsky, R. Jelinek, Gold nanoparticle self-assembly in two-component lipid Langmuir monolayers, Langmuir **27**, 1260 (2011).
[11] J. Paczesny, K. Sozański, I. Dzięcielewski, A.Żywociński, and R. Hołyst, Formation of net-like patterns of gold nanoparticles in liquid crystal matrix at the air-water interface, J. Nanopart. Res. **14**, 826 (2012).

[12] M. Choudhuri and A. Datta, A two-dimensional network of Au nanoclusters on water surface: Example of facile control of nanospace, J. Nanosci. Nanotechnol. **14**, 2901 (2014).

[13] Y. Zhao, G.C. Wang, T.M. Lu, *Experimental Methods in the Physical Sciences*, **37** (Academic Press, San Diego, USA), (2001).

[14] F.C. Moon, *Chaotic and Fractal Dynamics*, (WILEY-VCH Verlag GmbH and Co. KGaA, Weinheim), (2004).

[15] I. Prigogine and I. Stengers, *Order out of Chaos*, (Fontana Paperbacks), (1985).

[16] K. Kaneko, Pattern dynamics in spatio temporal chaos, Physica D **34**, 1 (1989).

[17] M. Brust, M.Walker, D. Bethell, D.J. Schiffrin, and R. Whyman, Synthesis of thiol- derivatised gold nanoparticles in a two phase liquid-liquid system, J. Chem. Soc. Chem. Commun., 801 (1994).

[18] W.P. Halperin, Quantum size effects in metal particles, Rev.Mod. Phy. **58**, 533 (1986).

[19] V. M. Kaganer, H. Möhwald, and P. Dutta, Structure and phase transitions in Langmuir monolayers, Rev. Mod. Phys. **71**, 779 (1999).

[20] C.M. Knobler and R.C. Desai, Phase transitions in monolayers, Ann. Rev. Phys. Chem. **43**, 207 (1992).

[21] M. K. Bera, M. K. Sanyal, S. Pal, J. Daillant, A. Datta, G. U. Kulkarni, D. Luzet and O. Konovalov, Reversible buckling in monolayer of gold nanoparticles on water surface, Europhys. Lett. **78**, 56003 (2007).

[22] B. Lin, D. G. Schultz , Xiao-Min Lin, Dongxu Li, J. Gebhardt, M. Meron , P.J. Viccaro, Langmuir monolayers of gold nanoparticles, Thin Solid Films **515**, 5669 (2007).

[23] D. Hönig and D. Möbius, Reflectometry at the Brewster angle and Brewster angle microscopy at the air-water interface, Thin Solid Films **210**, 64 (1992).

[24] S. Hénon and J. Meunier, Microscope at the Brewster angle: direct observation of first-order phase transitions in monolayers, Rev. Sci. Instrum. **62**, 936 (1991).

[25] A. Wolf, J. B. Swift, H. L. Swinney and J. A. Vastano, Determining Lyapunov exponents from a time series, Physica D **1**6, 285, (1985).

[26] M.T. Rosenstein, J.J. Collins and C.J. De Luca, A practical method for calculating largest Lyapunov exponents from small data sets, Physica D **65**, 117 (1993).

[27] R. Hegger, H. Kantz, T. Schrieber, Practical implementation of nonlinear time series methods: The TISEAN package, Chaos **9**, 413 (1999).

[28] J. Foisy, M. Alfaro, J. Brock, N. Hodges and J. Zimba, The standard double soap bubble in R^2 uniquely minimizes perimeter, Pacific J. Math. **159**, 47 (1993).

[29] R.E Peierls, Quelques proprits typiques des corps solides, Ann. Inst. Henri Poincaré **5**, 177 (1935).

[30] N.D. Mermin, Crystalline order in two dimensions, Phys. Rev. **176**, 250 (1968).

[31] P. Hohenberg, Existence of long-range order in one and two dimensions, Phys. Rev. **158**, 383 (1967).

[32] L.D Landau, Theory of phase transformations, Phys. Z. Sowjet. **11**, 26 (1937).

[33] T. Turiv, I. Lazo, A. Brodin, B.I. Lev, V. Reiffenrath, V.G. Nazarenko and O.D. Lavrentovich, Effect of collective molecular reorientations on Brownian motion of colloids in nematic liquid crystal, Science **342**, 1351 (2013).